# Benchmarking AlphaMissense Pathogenicity Predictions Against Cystic Fibrosis Variants

Eli Fritz McDonald[1,2], Kathryn E. Oliver[3], Jonathan P. Schlebach[4], Jens Meiler[1,2,5,6,*], Lars Plate[1,7,8*]

[1]Department of Chemistry, Vanderbilt University, Nashville, TN 37235, USA
[2]Center for Structural Biology, Vanderbilt University, Nashville, TN 37240, USA
[3]Department of Pediatrics, Emory University School of Medicine, Atlanta, GA 30322, USA
[4]Department of Chemistry, Purdue University, West Lafyette, IN 47907, USA
[5]Department of Pharmacology, Vanderbilt University, Nashville, TN 37240, USA
[6]Institute for Drug Discovery, Leipzig University, Leipzig, SAC 04103, Germany
[7]Department of Biological Sciences, Vanderbilt University, Nashville, TN 37235, USA
[8]Department of Pathology, Microbiology and Immunology, Vanderbilt University Medical Center, Nashville, TN 37232, USA

* Corresponding authors: JM (jens@meilerlab.org), LP (lars.plate@vanderbilt.edu)

**Abstract**

Mutations in cystic fibrosis transmembrane conductance regulator (CFTR) result in cystic fibrosis – a lethal genetic disease. Missense mutations that alter a single amino acid in the CFTR protein are among the most common cystic fibrosis mutations. AlphaMissense (AM) is a new technology that predicts the pathogenicity of missense mutations based on dual learned protein structure and evolutionary features. We evaluated the ability of AM to predict the pathogenicity of CFTR missense variants. AM predicted a high pathogenicity for CFTR residues overall, resulting in a high false positive rate and fair classification performance on CF variants from the CFTR2.org database. AM pathogenicity score correlated modestly with pathogenicity metrics from persons with CF including sweat chloride level, pancreatic insufficiency rate, and pseudomonas infection rate. Correlation was also modest with CFTR trafficking and folding competency *in vitro*. By contrast, the AM score correlated well with CFTR functional data *in vitro* – demonstrating the dual structure and evolutionary training approach learns important functional information despite lacking such data during training. Different performance across metrics indicated AM may determine if polymorphisms in CFTR are recessive CF variants yet cannot differentiate mechanistic effects or the nature of pathophysiology. Finally, AM predictions offered limited utility to inform on the pharmacological response of CF variants i.e., theratype. The development of new approaches to differentiate the biochemical and pharmacological properties of CF variants is therefore still needed to refine the targeting of emerging precision CF therapeutics.

## Introduction

Cystic fibrosis (CF) is a lethal genetic disease caused by variants in the epithelial anion channel cystic fibrosis transmembrane conductance regulator (CFTR)[1]. CFTR is composed of two nucleotide binding domains (NBDs), two transmembrane domains (TMDs) and an unstructured regulatory domain (RD)[2]. Loss of CFTR protein production or function results in osmotic dysregulation at the epithelium of the skin, pancreatic duct, and lungs – leading to high sweat chloride levels, pancreatic insufficiency, and lung infections respectively[3]. The current treatment paradigm for CF involves small molecule CFTR modulators known as *potentiators* and *correctors*. CFTR variants experience distinct structural defects and proteostasis states leading to divergent pharmacological response profiles to modulators also known as *theratype*[4].

Many CFTR variants are single amino acid substitutions or missense variants. Recently, AlphaMissense (AM) a technology designed to predict the pathogenicity of missense variants throughout the human proteome was published[5]. Among well-characterized genetic diseases, AM included CF pathogenicity predictions for every possible CFTR single amino acid substitution. AM provides a significant advance beyond previous attempts to model a limited number of CFTR variants[6,7]. Here, we evaluated the predictive validity of AM across several metrics of CF data such as pathogenicity in persons with CF, CFTR *in vitro* folding and fitness, and theratype.

The increasing pace of novel CFTR variant discovery has created a need for pathogenicity prediction, especially among wild type (WT) heterozygous individuals – carriers – whose mutations remain unknown. Our analysis suggests AM predicts the relative pathogenicity of severe CF-causing mutations well, while performing modestly on variants of variable clinical outcome and variants of unknown significance. Overall, AM showed a high false positive rate for predicting CFTR2 patient outcomes[8]. Two variants from the CFTR2 database and 368 variants from ClinVar[9] of unknown consequence were predicted as pathogenic. By contrast, variant of unknown consequence S912L from CFTR2 was predicted benign despite clinical outcome metrics characteristic of CF. AM scores correlated modestly with CF pathogenicity metrics and CFTR trafficking/folding competency *in vitro*. Correlation improved when compared to CFTR channel functional data. These analyses imply AM has learned important trends in variant function despite not training on such data. Finally, we provide evidence that AM offers little power in predicting CFTR variant theratype, although we note this measure is beyond its intended design. Thus, AM may offer capabilities in predicting pathogenicity of emerging variants but proved less useful for theratyping variants.

## Results and Discussion

### I. AlphaMissense predictions of CFTR pathogenicity

AM makes pathogenicity predictions based on a 90% accuracy against ClinVar data and thus derived different pathogenicity classification cut off values for individual proteins[5]. For CFTR, AM predicted scores from 0.56 – 1.00 as pathogenic, scores from 0.34 – 0.56 as ambiguous, and scores from 0.04 – 0.34 as benign. We mapped the average AM prediction score per residue onto a CFTR structure (PDBID 5UAK)[10] (**Figure 1A**). [10] (**Figure 1A**). The transmembrane domains showed a propensity for pathogenicity in contrast to residue conservation as calculated by ConSurf[11], which suggested the TMDs are comparatively variable across species (**Figure 1A & Supplemental Figure S1A**). Since the regulatory domain (RD) is disordered and not resolved in the CFTR structure 5UAK, we also plotted the AM average score for RD residues against a RD map highlighting key features such as transiently formed α-helices and phosphorylation sites[4] (**Figure 1B**). Despite noted difficulty with disordered regions[5], AM predicted RD residues ~760-775 as a hotspot for pathogenicity. This is consistent with the role of transient helix 752-778 in CFTR gating through interactions with a conserved region of the NBD2 C-terminus[12,13].

We sought to evaluate AM's ability to correctly predict CF pathogenesis on 169 missense variants from CFTR2.org[8]. The CFTR2 database offered a rich patient metric repository including pathogenicity classifications as CF causing, variable clinical consequence, or non-CF causing (**Supplemental Table 1**). We

calculated the receiver operating characteristic (ROC) curve for all pairwise comparisons of pathogenicity predicted by AM (**Figure 1C, See Methods**). Benign predictions showed the highest area under the curve (0.91) followed by pathogenic (0.80) and ambiguous respectively (0.66) – suggesting that AM has a high false positive rate particularly for ambiguous variants. We noted seven variants of unknown significance in the CFTR2.org database and their respective AM predictions (**Table 1**). Variants D924N and M952T, both located in transmembrane helix 8 (**Supplemental Figure S1B**), were predicted as pathogenic.

For performance comparison, we also plotted ROC curves for AM predictions of the 115 ClinVar classifications from the AlphaMissense study and observed 96% average accuracy as presented previously[5] (**Supplemental Figure S1C**). To validate this, we additionally downloaded a dataset of 219 variants directly from Clinvar, including 104 overlapping variants from the AlphaMissense benchmark set. The ROC curve for our Clinvar dataset showed >90% prediction accuracy with additional variants (**Supplemental Figure S1D**). In addition to classified variants used for performance evaluation, ClinVar contains 1277 CFTR variants of unknown significance[9]. AM predicted unknown consequence ClinVar variants to contain 728 benign, 181 ambiguous, and 368 pathogenic variants (**Supplemental Figure S1D, Supplemental Table 2**).

Previous analysis of CFTR variants across sampled genetic information suggested the NBD1/intercellular loop 4 (ICL4) interface as a hotspot of pathogenicity[14]. A heatmap of AM score was generated for NBD1 residues from 485-565 encompassing the α-helical subdomain, structurally diverse region, and the entire NBD1/ICL4 interface (**Figure 1D**). Of note, position 508 is intolerant to substitution. Deletion of F508 is the most frequent mutation in patients with CF. Although not directly interfacing with ICL4, residues 512-532 make up helix 4/4b of the α-helical subdomain and are relatively tolerant to variants except for V520 and C524. V520F was among variants characterized recently as non-responsive to clinical available modulators[7]. Residues 533-547 in the structurally diverse region are expectedly tolerant. By contrast, residues 548-565 make up the NBD1 core helix 5 that directly interfaces ICL4. This region is intolerant to substitution and contains many non-responsive variants such as R560T/K[4,14] (**Figure 1D**). We also generated a heatmap of AM scores for ICL4 residue 1048-1084 and revealed 1069 and 1072 as relatively tolerant to substitution amongst a comparatively intolerant region of CFTR (**Figure 1E**). Together, these data suggested AM pathogenicity scores matched previous findings and our general understanding about residue conservation throughout CFTR while providing specific information about every possible substitution.

## II. Cystic Fibrosis pathogenicity correlated modestly with AlphaMissense predictions

In addition to classifying variant pathogenicity, the CFTR2.org database annotates clinical data for persons with CF including sweat chloride levels, pancreatic insufficiency rates, pseudomonas infection rates, and lung function[8]. We curated the available patient data for 123 CFTR missense mutations (**Supplemental Table 1**) and analyzed ability of AM to predict patient pathogenicity metrics. Of note, CFTR2 data was based on individual alleles, e.g. missense variants.

First, we plotted AM score versus CF sweat chloride levels reported for 123 missense variants (**Figure 2A**). AM score correlated modestly with sweat chloride levels (Pearson Correlation Coefficient: 0.46, Spearman Correlation Coefficient: 0.48). CF causing variants, shown in blue, clustered in the top right corner indicative of high scores and high sweat chloride levels. By contrast, variable consequence variants, shown in yellow, clustered in the bottom right corner, indicating an excessive AM score (**Figure 2A**). Of note, variant of unknown significance S912L was predicted benign with a score of 0.12 but showed sweat chloride levels of 60 mEq/L – twice as high as healthy individuals (<30 mEq/L).

Next, we plotted AM score versus pancreatic insufficiency rates for 116 missense variants present on at least one allele of persons with CF (**Figure 2B**). AM scores correlated poorly with pancreatic insufficiency rates (Pearson coefficient: 0.31, Spearman Coefficient: 0.41) compared to sweat chloride. Again, AM failed to predict variable consequence variants, shown in yellow, on this metric (**Figure 2B**). Benign predicted variant S912L shows a 57% pancreatic insufficiency rate.

Finally, we plotted AM score versus pseudomonas infection rates for 114 missense variants on at least one allele (**Figure 2C**). AM correlated better with pseudomonas infection than pancreatic insufficiency rates, but worse than sweat chloride (Pearson Coefficient: 0.38, Spearman Coefficient: 0.44). However, it performed

better on variable consequence variants. Once again, the benign predicted variant of unknown significance S912L shows a 50% pseudomonas infection rate – suggesting this variant may present more pathologically than predicted or annotated by CFTR2 (**Figure 2C**). Of note, pathogenic predicted variants D924N and M952T have insufficient data available on CFTR2 for comparison. In summary, AlphaMissense correlated modestly with clinical data specifically performing poorly on variants of variable consequence. The heterozygous allele problem and high false positive rate likely contributed to poor performance. Patients can be heterozygous and may have different CFTR variants on each allele. This may bias clinical data, as heterozygous persons with CF with different severity variants on each allele (e.g. CF causing, and variable) would have different outcomes than heterozygous persons with CF with the same severity on each allele (e.g. two CF causing).

## III. AlphaMissense predicts CFTR fitness beyond folding and trafficking competency

Much *in vitro* functional data about CFTR variants is also available for comparison, including recent deep mutational scanning (DMS) and variant drug response screening studies[7,15]. In the DMS study, fluorescence activated cell sorting was used to measure the cell surface immunostaining intensity of a epitope-tagged library of 129 CFTR variants including 100 missense variants[7]. In the drug response study, 650 variants including 585 missense variants were screened for their trafficking efficiency and function[15].

First, we evaluated AM ability to predict CFTR folding competency – which is well characterized to correlate with cell surface expression and trafficking efficiency[16–19]. We plotted AM prediction scores for 100 missense variants versus DMS cell immune-staining intensity (**Figure 3A**), which showed an inverse relationship but correlated poorly (Pearson coefficient: -0.37, Spearman Coefficient: -0.37). Notably, among variants in the top right corner, e.g. high AM score and high surface staining, we observed several gating mutations (G551D/S, R347H, S1251N, G1244E etc.), which traffic well in HEK293T cellsbut still cause CF (**Figure 3A**). This result demonstrated that AM performed poorly on inferring the nature of the variant defect.

Next, we plotted AM prediction scores for 538 missense variants versus CFTR trafficking efficacy as measured by the mature CFTR to immature CFTR ratio - C/B band ratio on western blot (**Figure 3B**)[15]. Experimental data was filtered for plotting clarity (**Supplemental Figure 2, See Methods**). AM scores displayed improved inverse correlation with the larger trafficking efficiency dataset (Pearson coefficient: -0.50, Spearman Coefficient: -0.53) suggesting AM can predict CFTR folding competency across a variety of types of variants. Several off-axis variants were noted which show poor predictions as well as <30% WT trafficking based on distribution of all trafficking data (**Supplemental Figure 2A-B**).

Finally, we evaluated AM ability to predict CFTR fitness as measured by transepithelial current clamp conductance[15]. We plotted AM prediction scores versus forskolin-induced basal CFTR channel activity as percent WT (FSK %WT) for 546 missense variants (**Figure 3C**). AM scores inversely correlated best with CFTR function (Pearson coefficient: -0.70, Spearman Coefficient: -0.69). Several off-axis variants were noted which show poor predictions and <30% WT function based on the distribution of functional data (**Supplemental Figure 2C-D**). Together these analyses indicated that AM scores are closely aligned with pathogenicity but cannot differentiate between mutations that compromise expression versus function.

## IV. AlphaMissense cannot predict CFTR variant theratype

There remains an unmet need for rational selection of cystic fibrosis therapies as novel variants emerge from genetic screening and novel modulators emerge from clinical trials. CFTR variant theratyping has been an intense area of study in CF[20,21]. We were curious if AM offered any predictive power for CFTR theratyping, although we note this task is outside its intended design. To determine potential use, theratype distinguishing plots were generated and colored by AM pathogenicity score to see if any obvious patterns arose. We split the VX-445 sensitive variants from VX-661 sensitive variants along a diagonal axis best fit by plotting CFTR immune staining intensity for VX-445 versus VX-661 (**Figure 4A**). VX-445 sensitive variants fell above the dotted line and VX-661 variants fell below the dotted line[7]. The variants were then colored by AM pathogenicity score. The distribution of colors across the responsive spectrum revealed little discernable pattern

(**Figure 4A**). Likewise, we plotted basal CFTR immune staining intensity versus VX-661, VX-445, and combination treatment VX-661 + VX-445 and colored variants by their AM pathogenicity score (**Supplemental Figure 3A-C**). Again, AM score colors showed little pattern and appear distributed randomly.

Next, we used the drug response study CFTR functional data* and plotted the VX-445 + VX-661 FSK (%WT) CFTR activity versus basal activity and colored by AM pathogenicity score (**Figure 4B**). Benign variants fell along a linear diagonal and suggested that benign predicted variants all experience a linear response to CFTR correctors. We speculate this response may reflect well documented WT modulator response and implied a response inherent in the stabilizing effects of VX-445 and VX-661. C-B band ratio response colored by AM score portrayed a random distribution of score color (**Supplemental Figure 4A**). Pathogenic predicted variants in both plots show a random distribution. To determine if variant location combined with score predicted theratype we split the plot in **Figure 4B** by domain (**Supplemental Figure 4B-E**). Each domain individually showed a similar random distribution of score colors. Finally, we calculated relative degree CFTR correction by subtracting basal FSK (%WT) from VX-445+VX-661 correction FSK (%WT) and plotted this difference against AM score (**Figure 4C**). Again, no obvious pattern was observed. In summary, we found AM score afforded little predictive power for theratyping. However, AM score could potentially be a useful machine learning feature for future theratype prediction methods.

## Conclusion

AlphaMissense has the exciting potential to aid with pathogenicity classification of rare and emerging variants identified during genetic screening. CF posited a valuable case study for evaluating AM performance because of abundance of clinical outcome data and *in vitro* variant classifications available. AM predicted pathogenicity of severe CF-causing variants well, albeit with a high false positive rate and matched previous studies of CFTR variant pathogenicity in the NBD1/ICL4 interface[14]. However, AM performed modestly on variants with less disease severity and variable clinical consequence, and it offered little power in predicting theratype. Again, for pathogenic missense variants, AM score correlated modestly with processing defective (e.g. class II) and correlated well with functionally defective (e.g. class III) variants. Thus, predictions offer little information for distinguishing pathogenicity mechanism. AM may provide guidance in determining if polymorphisms in CFTR are recessive CF variants, but performance on less severe disease variants indicate that caution must be taken when interpreting AM predictions. *In vitro* measurements on variant severity may aid in evaluating prediction quality and will additionally remain necessary for CFTR theratyping.

## Methods

*Data Curation and Collection*

AlphaMissense (AM) predictions for all single amino acid substitutions in the human proteome data was downloaded, gunzipped, and searched using vim text editor for CFTR accession number/Uniprot ID P13569. CFTR AM predictions were extracted into a separate file for analysis. Cystic Fibrosis patient data was initially downloaded from the Variant List History tab on CFTR2.org. The table of 804 variants was filtered for 178 missense variants by removing in/dels, splicing variants, premature stop codons, etc. The patient information was manually curated by searching each mutation and annotating the sweat chloride (mEq/L), pancreatic insufficiency rate (%), pseudomonas infection rate (%), lung function ages < 10 (FEV1%), lung function ages 10<20 (FEV1%), lung function ages >20 (FEV1%) (**Supplemental Table 1**). Lung function data proved too highly variable for comparison and was not used, but was still included in the Supplemental Table for reference. *In vitro* modulator response data was downloaded from[15] and Deep Mutational Scanning data downloaded from[7]. The 650 variants from[15] were filtered to 585 missense variants. ClinVar data was downloaded after searching for CFTR. Clinvar predictions were filtered for missense variants by removing, in/dels, stop codons, double missense variants, etc. Filtering yielded 1768 missense variant pathogenicity predictions (**Supplemental Table 2**). For performance comparison, the missense variants were filtered by clinical significance. We removed classifications such as *no interpretation*, *conflicting interpretations*, *uncertain significance*, and *drug response*. This left 219 variants classified as *pathogenic* or *likely benign* for performance evaluation and ROC plotting.

*Filtering Experimental Data*

Experimental data from Bihler et al.[15] were filtered to exclude highly variable data based on the SEM due to lack of reproducibility. We plotted both the distribution of the data itself to look for outliers on the y axis of our correlation plots (**Figure 3B-C**) and the distribution of the SEM (**Supplemental Figure 2**). We labeled outliers with a C-B ratio of less than 30, but with a benign AM prediction of less than 0.3 (**Supplemental Figure 2A, Figure 3B**). C-B band ratio SEM of greater than 30 were excluded from the analysis and not plotted for clarity, leaving 538 variants for analysis – 92% of the experimental data (**Supplemental Figure 2B**). For the functional data, we labeled outliers of interest with a FSK %WT of less than 30, but with a benign AM prediction of less than 0.3 (**Supplemental Figure 2C, Figure 3C**). FSK %WT SEM of greater than 20 were excluded from the analysis and not plotted for clarity, leaving 546 variants for analysis – 93% of the available experimental data.

*Analysis*

Data were analyzed and plotted in Python 3. Raw excel files were imported and parsed using the Pandas data frame library and plots were generated with the matplotlib.pyplot and seaborn libraries. Pearson and Spearman correlation coefficients were calculated with the scipy.stats library using the pearsonr() and spearmanr() functions respectively. Plots were generated for all possible variants with available data for a given metric. The receiver operating characteristic (ROC) curve for AM pathogenicity predicted by AM was calculated against CFTR2 classification. CFTR2 classifies variants as CF causing, variable clinical consequence, or non-CF causing. We equated the AM prediction pathogenic to CF causing, ambiguous to variable, and benign to non-CF causing. Since ROC is used for binary classification, all pairwise comparisons were considered. In each ROC curve, a different prediction (pathogenic, ambiguous, or benign) was taken to be a true positive, and the other two predictions to be false positives. Then the corresponding true positive and false positive rates were calculated by considering all possible score cutoffs for pathogenicity. Theratype discerning plots were generated to distinguish responsive from non-responsive variants graphically and colored by the variants respective AM score.

## Acknowledgments

This work was supported by R35 GM133552 (NIGMS), R01 HL167046 (NHBLI), R00HL151965 (NIH) and OLIVER22A0-KB (CFF). EFM was supported by a predoctoral fellowship F31 HL162483 (NHLBI) and Chemical-Biology Interface training grant T32 GM065086 (NIGMS).

## Author Contributions

Conceptualization: E.F.M., L.P. Funding acquisition: E.F.M., K.E.O., J.P.S., L.P., J.M. Data Collection: E.F.M., K.E.O. Data Analysis: E.F.M. Writing original draft: E.F.M.; Writing review and editing, E.F.M., J.M., L.P. All authors have read and agreed to the published version of the manuscript.

## Figures

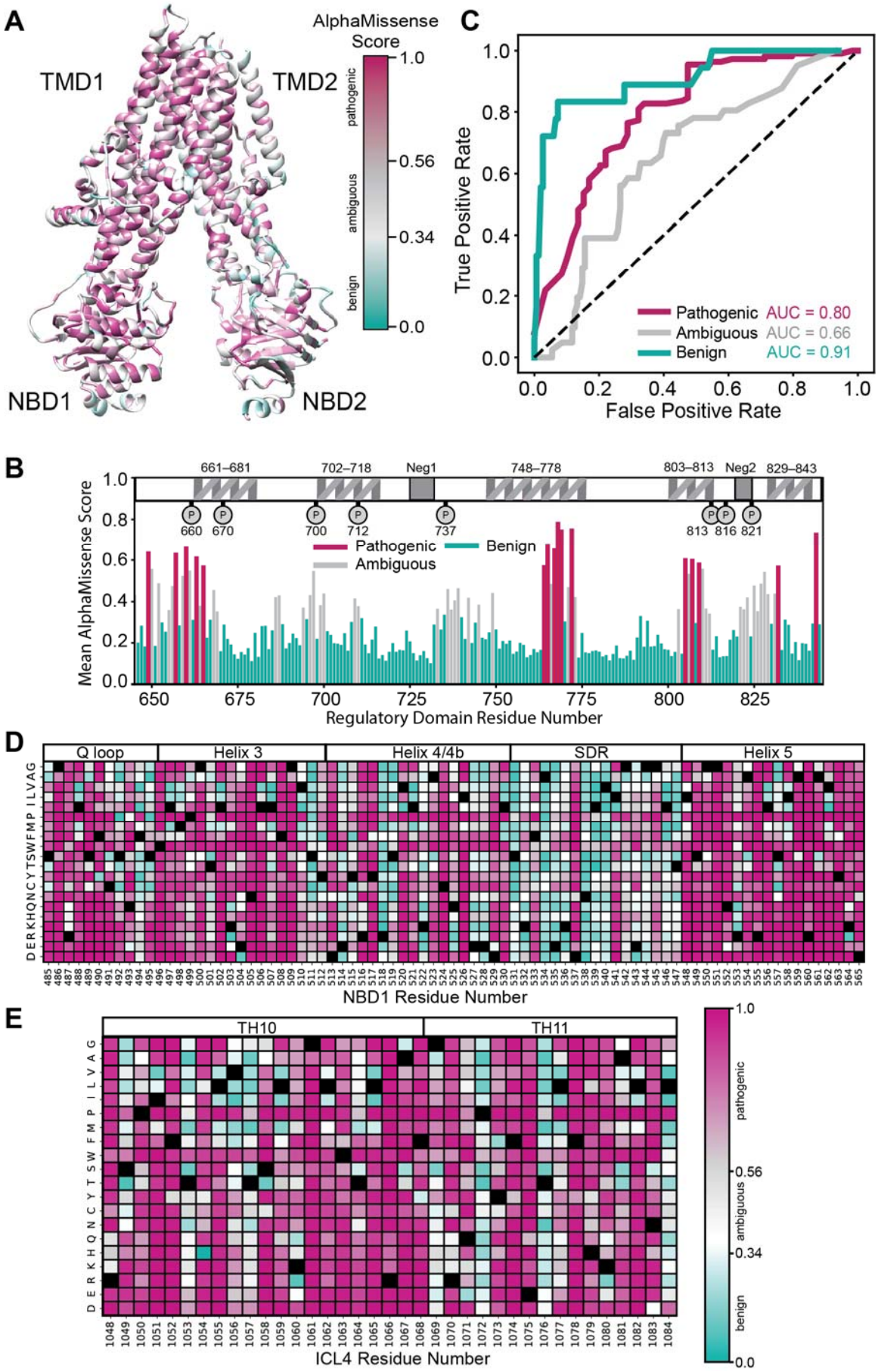
A
TMD1
TMD2
NBD1
NBD2
AlphaMissense Score
pathogenic
ambiguous
benign
1.0
0.56
0.34
0.0
C
True Positive Rate
False Positive Rate
Pathogenic AUC = 0.80
Ambiguous AUC = 0.66
Benign AUC = 0.91
B
661–681
702–718
Neg1
748–778
803–813
Neg2
829–843
Mean AlphaMissense Score
Pathogenic
Ambiguous
Benign
Regulatory Domain Residue Number
D
Q loop
Helix 3
Helix 4/4b
SDR
Helix 5
NBD1 Residue Number
E
TH10
TH11
ICL4 Residue Number

**Figure 1. AlphaMissense predictions of CFTR pathogenicity compared to CFTR2.org repository**

**A.** The average AM score per residue mapped onto the CFTR structure (PDBID 5uak)[4]. Variants with a score from 0.56-1.00 were classified by AM as pathogenic, variants with a score from 0.34 - 0.56 were classified as ambiguous, and variants with a score from 0.04 – 0.34 were classified as benign.

**B.** The average AM score for the regulatory domain (RD) with an RD map of important features for reference[4]. Transient helices shown, two negatively charged regions (Neg1/2), and important phosphorylation sites shown as P. Notably, the second half of the transient helix 748-778 is predicted to be a hotspot of RD variant pathogenicity.

**C.** Receiver operating characteristic (ROC) curve of AM predictions benchmarked against 169 CFTR2.org database classifications. Our curated data set contained 110 CF causing, 41 variable clinical consequence, and 18 non-CF causing missense variants. In the pathogenic curve (violet) – pathogenic prediction of a CF causing mutation was considered a true positive. Likewise in the ambiguous curve (grey) – ambiguous prediction of a variable clinical outcomes was considered a true positive. Finally, in the benign curve (bluegreen) – benign prediction of a non-CF causing variant was considered a true positive.

**D.** Heatmap of AM scores for NBD1 residues 485-565 including all regions interfacing with ICL4 and adjacent regions. Pathogenicity colored as in **A.** and WT residues depicted in black.

**E.** Heatmap of AM scores for ICL4 residues 1048-1084, colored as in **E.**

| Variant | AlphaMissense Score | Pathogenicity Prediction |
|---|---|---|
| R31L | 0.17 | benign |
| V201M | 0.36 | ambiguous |
| A349V | 0.26 | benign |
| S912L | 0.12 | benign |
| D924N | 0.83 | pathogenic |
| M952T | 0.85 | pathogenic |
| Y1014C | 0.37 | ambiguous |

**Table 1. CFTR2.org Variants of Unknown Consequence** Seven missense variants of unknown significance from the CFTR2.org database with their respective AM scores and predicted pathogenicity. Mutations D923N and M952T are predicted to be pathogenic.

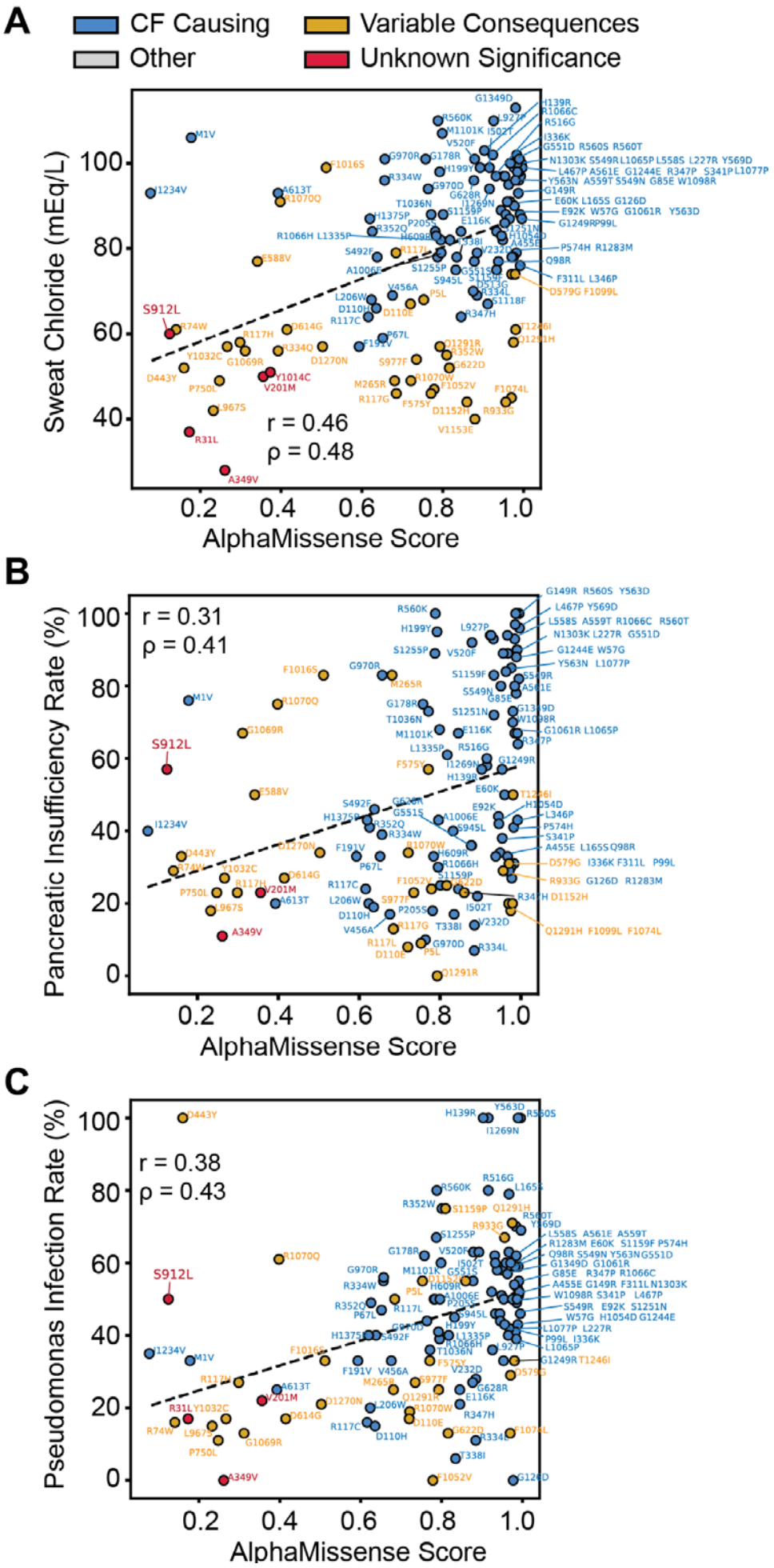
A
CF Causing
Variable Consequences
Other
Unknown Significance
Sweat Chloride (mEq/L)
AlphaMissense Score
r = 0.46
ρ = 0.48
B
Pancreatic Insufficiency Rate (%)
AlphaMissense Score
r = 0.31
ρ = 0.41
C
Pseudomonas Infection Rate (%)
AlphaMissense Score
r = 0.38
ρ = 0.43

**Figure 2. Benchmarking AlphaMissense against Cystic Fibrosis patient pathogenicity metrics**

**A.** AM score plotted against sweat chloride levels in milliequivalents per liter (mEq/L) for 123 missense mutations. Healthy sweat chloride levels were <30 mEq/L. CF causing mutations were shown in blue, mutations were variable consequence were shown in yellow, and variants of unknown significance were shown in red (as annotated in CFTR2). A modest linear correlation (Pearson Coefficient $r = 0.46$, Spearman Coefficient $\rho = 0.48$) was observed.

**B.** AM score plotted against pancreatic insufficiency rates in percent for 116 missense mutations. Less correlation (Pearson Coefficient $r = 0.31$, Spearman Coefficient $\rho = 0.41$) was observed than with sweat chloride, notably many variable consequence variants were predicted pathogenic AM score but demonstrate a low pancreatic insufficiency rate. Colors annotated as in **A.**

**C.** AM score plotted against pseudomonas infection rates in percent for 114 missense mutations. Colors annotated as in **A.** Linear correlation (Pearson Coefficient $r = 0.38$, Spearman Coefficient $\rho = 0.43$) is shown. Interestingly, S912L, a variant of unknown significance is predicted to be benign but shows a high sweat chloride, pancreatic sufficiency, and pseudomonas infection rate compared to variants with similar scores.

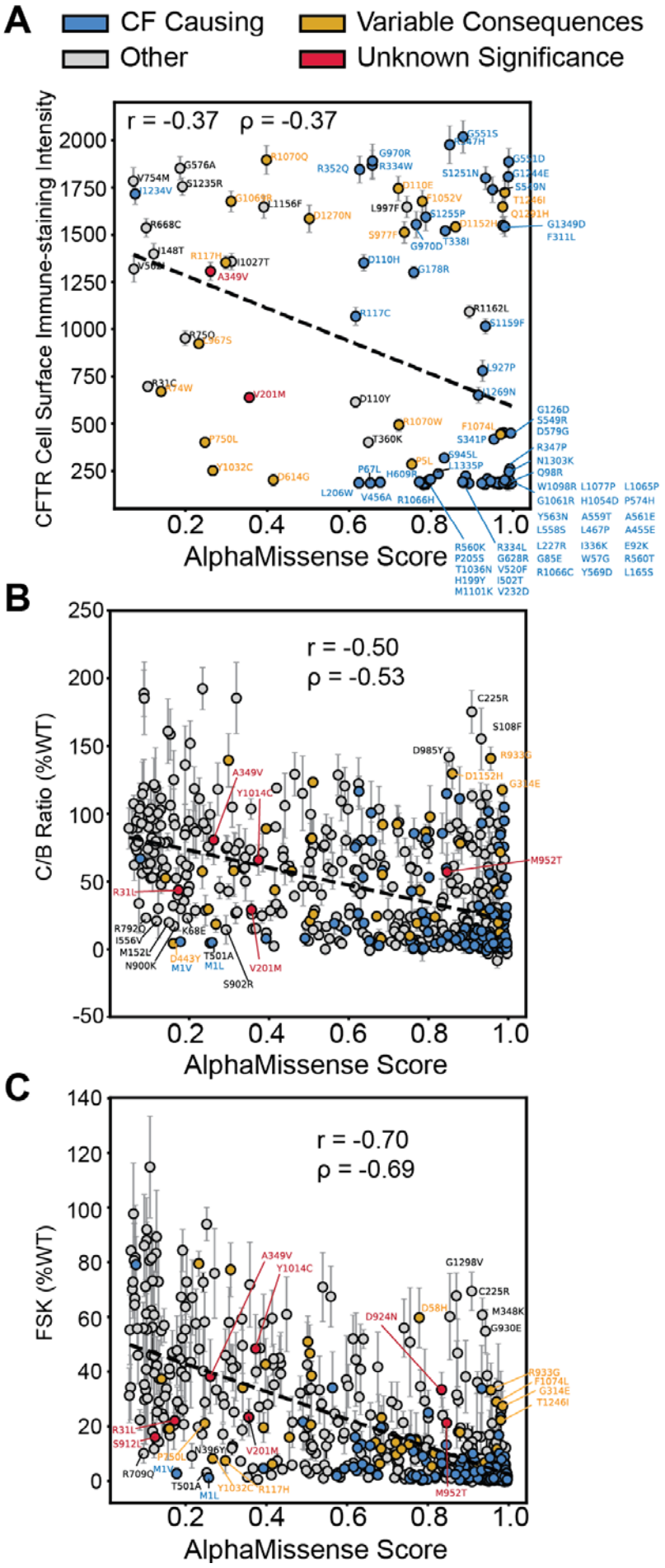
A
CF Causing
Variable Consequences
Other
Unknown Significance
r = -0.37 ρ = -0.37
CFTR Cell Surface Immune-staining Intensity
AlphaMissense Score
B
r = -0.50
ρ = -0.53
C/B Ratio (%WT)
AlphaMissense Score
C
r = -0.70
ρ = -0.69
FSK (%WT)
AlphaMissense Score

**Figure 3. Benchmarking AlphaMissense against CFTR *in vitro* fitness metrics**

**A.** AM score plotted against Deep Mutational Scanning data for 100 missense variants in HEK293T cells[7]. Y axis represents the cell surface immune-staining intensity of CFTR and thus is indicative of the CFTR trafficking levels to the cell surface. A slight inverse linear correlation was observed (Pearson Coefficient r = -0.37, Spearman Coefficient ρ = -0.37). Some off axis variants such as G551D are gating mutations and thus fail to experience aberrant trafficking in the HEK293T cell background but still exhibit impaired channel function. CF causing mutations are shown in blue, mutations of variable consequence are shown in yellow, and variants of unknown significance are shown in red (as annotated in CFTR2).

**B.** AM score plotted against CFTR western blot C-B band ratio in percent WT for 538 missense mutations[15]. Several off-axis mutations are highlighted. Color annotation as in **A.** Inverse linear correlation (Pearson Coefficient r = -0.50, Spearman Coefficient ρ = -0.53) improves for this larger dataset. Of note, variants of unknown significance D924N and S912L were filtered out of this dataset due an SEM >30, indicative of poor reproducibility across replicates (**Supplemental Figure 2A-B**).

**C.** AM score plotted against Forskolin induced CFTR current in percent WT for 546 missense mutations[15]. Color annotation as in **A.** Inverse linear correlation (Pearson Coefficient r = -0.70, Spearman Coefficient ρ = -0.69) is higher the function data compared to trafficking alone. All seven CFTR2 variants of unknown significance are highlighted.

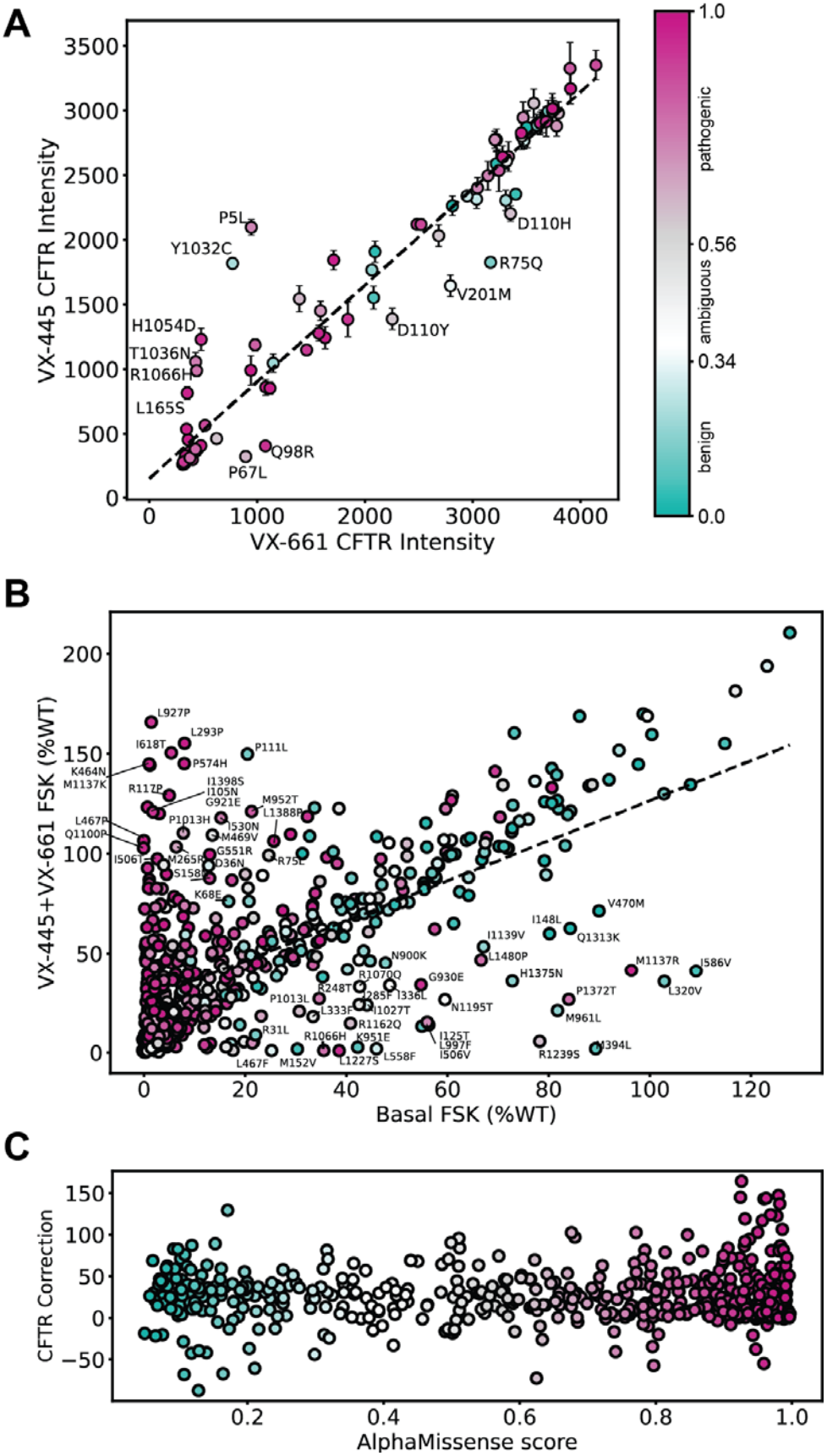


**Figure 4. CFTR theratype plots colored by AlphaMissense pathogenicity score.**
**A.** CFTR cell surface immune staining intensity comparing treatment with VX-661 versus VX-445 correctors with the dotted line representing equivalent response to both correctors[7] . Variants that fell below the best fit

dotted line are selectively responsive to VX-661 while variants above the dotted line were selectively responsive to VX-445. The AlphaMissense pathogenicity predictions (color gradient) show no correlation with the corrector response patterns for CFTR variants. Variants with a score from 0.56-1.00 were classified by AM as pathogenic (violet), variants with a score from 0.34 - 0.56 were classified as ambiguous (grey), and variants with a score from 0.04 – 0.34 were classified as benign (green). Error bars represent standard deviation of the cell surface immunostaining intensity. Selectively sensitive variants were annotated.

**B.** Correlation of the basal CFTR activity versus CFTR activity when treated with dual corrector combination (VX-445, VX-661) from[15]. FSK-induced CFTR channel activity is expressed as % WT. Error bars were excluded for clarity and AM predicted pathogenicity colored as in **A.** A line of benign variants emerged suggesting thatAM benign predicted mutations display a similar response to correctors that is dependent on the their basal activity. Pathogenic variants, by contrast, showed little pattern or ability to predict theratype. Off axis variants were annotated.

**C.** Degree of functional CFTR correction was calculated by subtracting basal FSK (%WT) levels from VX-445+VX-661 FSK (%WT) levels and then plotted against AM score and colored by score. CFTR variants across the continuum of AM scores displayed variable functional response to the corrector combination. AM predicted pathogenicity colored as in **A.**

## References


(1) Welsh, M. J.; Smith, A. E. Molecular Mechanisms of CFTR Chloride Channel Dysfunction in Cystic Fibrosis. *Cell* **1993**, *73* (7), 1251–1254. https://doi.org/10.1016/0092-8674(93)90353-R.

(2) Riordan, J. R.; Rommens, J. M.; Kerem, B.-S.; Alon, N.; Rozmahel, R.; Grzelczak, Z.; Zielenski, J.; Lok, S.; Plavsic, N.; Chou, J.-L.; Drumm, M. L.; Iannuzzi, M. C.; Collins, F. S.; Tsui, L.-C. Identification of the Cystic Fibrosis Gene: Cloning and Characterization of Complementary DNA. *Science* **1989**, *245* (4922), 1066–1073. https://doi.org/10.1126/science.2475911.

(3) Cutting, G. R. Cystic Fibrosis Genetics: From Molecular Understanding to Clinical Application. *Nat. Rev. Genet.* **2015**, *16* (1), 45–56. https://doi.org/10.1038/nrg3849.

(4) McDonald, E. F.; Meiler, J.; Plate, L. CFTR Folding: From Structure and Proteostasis to Cystic Fibrosis Personalized Medicine. *ACS Chem. Biol.* **2023**, acschembio.3c00310. https://doi.org/10.1021/acschembio.3c00310.

(5) Cheng, J.; Novati, G.; Pan, J.; Bycroft, C.; Žemgulytė, A.; Applebaum, T.; Pritzel, A.; Wong, L. H.; Zielinski, M.; Sargeant, T.; Schneider, R. G.; Senior, A. W.; Jumper, J.; Hassabis, D.; Kohli, P.; Avsec, Ž. Accurate Proteome-Wide Missense Variant Effect Prediction with AlphaMissense. *Science* **2023**, eadg7492. https://doi.org/10.1126/science.adg7492.

(6) McDonald, E. F.; Woods, H.; Smith, S. T.; Kim, M.; Schoeder, C. T.; Plate, L.; Meiler, J. Structural Comparative Modeling of Multi-Domain F508del CFTR. *Biomolecules* **2022**, *12* (3), 471. https://doi.org/10.3390/biom12030471.

(7) McKee, A. G.; McDonald, E. F.; Penn, W. D.; Kuntz, C. P.; Noguera, K.; Chamness, L. M.; Roushar, F. J.; Meiler, J.; Oliver, K. E.; Plate, L.; Schlebach, J. P. General Trends in the Effects of VX-661 and VX-445 on the Plasma Membrane Expression of Clinical CFTR Variants. *Cell Chem. Biol.* **2023**, *30* (6), 632-642.e5. https://doi.org/10.1016/j.chembiol.2023.05.001.

(8) The Clinical and Functional TRanslation of CFTR (CFTR2); Available at Http://Cftr2.Org.

(9) Landrum, M. J.; Lee, J. M.; Benson, M.; Brown, G. R.; Chao, C.; Chitipiralla, S.; Gu, B.; Hart, J.; Hoffman, D.; Jang, W.; Karapetyan, K.; Katz, K.; Liu, C.; Maddipatla, Z.; Malheiro, A.; McDaniel, K.; Ovetsky, M.; Riley, G.; Zhou, G.; Holmes, J. B.; Kattman, B. L.; Maglott, D. R. ClinVar: Improving Access to Variant Interpretations and Supporting Evidence. *Nucleic Acids Res.* **2018**, *46* (D1), D1062–D1067. https://doi.org/10.1093/nar/gkx1153.

(10) Liu, F.; Zhang, Z.; Csanády, L.; Gadsby, D. C.; Chen, J. Molecular Structure of the Human CFTR Ion Channel. *Cell* **2017**, *169* (1), 85–92. https://doi.org/10.1016/j.cell.2017.02.024.

(11) Ashkenazy, H.; Abadi, S.; Martz, E.; Chay, O.; Mayrose, I.; Pupko, T.; Ben-Tal, N. ConSurf 2016: An Improved Methodology to Estimate and Visualize Evolutionary Conservation in Macromolecules. *Nucleic Acids Res.* **2016**, *44* (W1), W344–W350. https://doi.org/10.1093/nar/gkw408.

(12) Naren, A. P.; Cormet-Boyaka, E.; Jian Fu, 1 Matteo Villain; Blalock, J. E.; Quick, M. W.; Kirk, K. L. CFTR Chloride Channel Regulation by an Interdomain Interaction. *Science* **1999**, *286* (October), 544–548.

(13) Bozoky, Z.; Krzeminski, M.; Muhandiram, R.; Birtley, J. R.; Al-Zahrani, A.; Thomas, P. J.; Frizzell, R. A.; Ford, R. C.; Forman-Kay, J. D. Regulatory R Region of the CFTR Chloride Channel Is a Dynamic Integrator of Phospho-Dependent Intra- and Intermolecular Interactions. *Proc. Natl. Acad. Sci. U. S. A.* **2013**, *110* (47). https://doi.org/10.1073/pnas.1315104110.

(14) Molinski, S. V.; Shahani, V. M.; Subramanian, A. S.; MacKinnon, S. S.; Woollard, G.; Laforet, M.; Laselva, O.; Morayniss, L. D.; Bear, C. E.; Windemuth, A. Comprehensive Mapping of Cystic Fibrosis Mutations to CFTR Protein Identifies Mutation Clusters and Molecular Docking Predicts Corrector Binding Site. *Proteins Struct. Funct. Bioinforma.* **2018**, *86* (8), 833–843. https://doi.org/10.1002/prot.25496.

(15) Bihler, H.; Sivachenko, A.; Millen, L.; Bhatt, P.; Patel, A. T.; Chin, J.; Bailey, V.; Musisi, I.; LaPan, A.; Allaire, N. E.; Conte, J.; Simon, N. R.; Magaret, A. S.; Raraigh, K. S.; Cutting, G. R.; Skach, W. R.; Bridges, R. J.; Thomas, P. J.; Mense, M. In Vitro *Modulator Responsiveness of 655* CFTR *Variants Found in People With CF*; preprint; Pharmacology and Toxicology, 2023. https://doi.org/10.1101/2023.07.07.548159.

(16) Mendoza, J. L.; Schmidt, A.; Li, Q.; Nuvaga, E.; Barrett, T.; Bridges, R. J.; Feranchak, A. P.; Brautigam, C. A.; Thomas, P. J. Requirements for Efficient Correction of Δf508 CFTR Revealed by Analyses of Evolved Sequences. *Cell* **2012**, *148* (1–2), 164–174. https://doi.org/10.1016/j.cell.2011.11.023.

(17) Rabeh, W. M.; Bossard, F.; Xu, H.; Okiyoneda, T.; Bagdany, M.; Mulvihill, C. M.; Du, K.; di Bernardo, S.; Liu, Y.; Konermann, L.; Roldan, A.; Lukacs, G. L. Correction of Both NBD1 Energetics and Domain Interface Is Required to Restore ΔF508 CFTR Folding and Function. *Cell* **2012**, *148* (1–2), 150–163. https://doi.org/10.1016/j.cell.2011.11.024.

(18) Protasevich, I.; Yang, Z.; Wang, C.; Atwell, S.; Zhao, X.; Emtage, S.; Wetmore, D.; Hunt, J. F.; Brouillette, C. G. Thermal Unfolding Studies Show the Disease Causing F508del Mutation in CFTR Thermodynamically Destabilizes Nucleotide-Binding Domain 1. *Protein Sci.* **2010**, *19* (10), 1917–1931. https://doi.org/10.1002/pro.479.

(19) He, L.; Aleksandrov, L. A.; Cui, L.; Jensen, T. J.; Nesbitt, K. L.; Riordan, J. R. Restoration of Domain Folding and Interdomain Assembly by Second□site Suppressors of the ΔF508 Mutation in CFTR. *FASEB J.* **2010**, *24* (8), 3103–3112. https://doi.org/10.1096/fj.09-141788.

(20) Clancy, J. P.; Cotton, C. U.; Donaldson, S. H.; Solomon, G. M.; VanDevanter, D. R.; Boyle, M. P.; Gentzsch, M.; Nick, J. A.; Illek, B.; Wallenburg, J. C.; Sorscher, E. J.; Amaral, M. D.; Beekman, J. M.; Naren, A. P.; Bridges, R. J.; Thomas, P. J.; Cutting, G.; Rowe, S.; Durmowicz, A. G.; Mense, M.; Boeck, K. D.; Skach, W.; Penland, C.; Joseloff, E.; Bihler, H.; Mahoney, J.; Borowitz, D.; Tuggle, K. L. CFTR Modulator Theratyping: Current Status, Gaps and Future Directions. *J. Cyst. Fibros.* **2019**, *18* (1), 22–34. https://doi.org/10.1016/j.jcf.2018.05.004.

(21) McDonald, E. F.; Sabusap, C. M. P.; Kim, M.; Plate, L. Distinct Proteostasis States Drive Pharmacologic Chaperone Susceptibility for Cystic Fibrosis Transmembrane Conductance Regulator Misfolding Mutants. *Mol. Biol. Cell* **2022**, *33* (7), ar62. https://doi.org/10.1091/mbc.E21-11-0578.